*J. Plasma Phys.* (2022), *vol*. 88, 175880301  
Published by Cambridge University Press
doi:10.1017/S0022377822000423

# Multiscale magnetic field structures in an expanding elongated plasma cloud with hot electrons subject to an external magnetic field

**M.A. Garasev [1], A.A. Nechaev [1], A.N. Stepanov [1], V.V. Kocharovsky [2] and Vl.V. Kocharovsky [1,†]**

[1]Institute of Applied Physics, Russian Academy of Sciences, Nizhny Novgorod 603950, Russia

[2]Department of Physics and Astronomy, Texas A&M University, College Station, TX 77843, USA

(Received 9 December 2021; revised 29 April 2022; accepted 29 April 2022)

We carry out three-dimensional and two-dimensional particle-in-cell simulations of the expansion of a magnetized plasma that initially uniformly fills a half-space and contains a semicylindrical region of heated electrons elongated along the surface of the plasma boundary. This geometry is related, for instance, to ablation of a plane target by a femtosecond laser beam under quasi-cylindrical focusing. We find that a decay of the inhomogeneous plasma–vacuum discontinuity is strongly affected by an external magnetic field parallel to its boundary. We observe various transient phenomena, including an anisotropic scattering of electrons and an accompanying Weibel instability, and reveal various spatial structures of the arising magnetic field and current, including multiple flying-apart filaments of a Z-pinch type and slowly evolving current sheets with different orientations. The magnitude of the self-generated magnetic field can be of the order of, or significantly exceed that of, the external one. Such phenomena are expected in the laser and cosmic plasmas, including the explosive processes in the planetary magnetospheres and stellar coronal arches.

**Key words:** plasma nonlinear phenomena, plasma simulation, plasma instabilities

## 1. Introduction

The problem of generation and coexistence of large- and small-scale magnetic fields during the expansion of a non-equilibrium collisionless plasma with hot electrons into a cold background plasma or vacuum is typical for many situations in the laboratory and cosmic plasma physics, including the phenomena of laser ablation, dynamics of the planetary magnetosheath regions, evolution of the solar (stellar) flares and wind formation (see, e.g. Medvedev & Loeb 1999; Gruzinov 2001; Lyubarsky & Eichler 2006; Romagnani *et al.* 2008; Spitkovsky 2008; Quinn *et al.* 2012; Huntington *et al.* 2015; Garasev & Derishev 2016; Sakawa *et al.* 2016; Göde *et al.* 2017; Balogh *et al.* 2018; Huang, Takabe & Cowan 2019; Srivastava *et al.* 2019; Ruyer *et al.* 2020). A plasma discontinuity or a transition layer could be inhomogeneously heated and exposed to an external magnetic field comparable in magnitude to the self-generated one and oriented at various angles

† Email address for correspondence: kochar@ipfran.ru

relative to the direction of the plasma density gradient or the axis of a plasma anisotropy induced by the expansion of a hot electron cloud.

We consider a particular, though quite typical, case of a plasma uniformly filling a half-space with a semicylindrical region of heated (Maxwellian) electrons elongated along the surface of the plasma boundary. This case is relevant, for example, to the expansion of a laser plasma produced by a femtosecond laser beam under quasi-cylindrical focusing on a plane target or the injection of a current filament with hot electrons into the upper part of a stellar coronal arch. By means of three-dimensional (3-D) and two-dimensional (2-D) particle-in-cell (PIC) simulations, we describe the inhomogeneous plasma flow and the evolution of the current structures of different scales, paying particular attention to the anisotropic cooling of electrons and the interplay between the self-generated and external magnetic fields in the dynamics of particles.

We resolve the formation of the stratified plasma flows and current sheets or filaments with dimensions of the order of or less than the particle gyroradius, i.e. the structures of a kinetic origin and reduced dimensionality, which are responsible for a small-scale stratification of the plasma. These structures and an accompanying reconnection of the magnetic field lines cannot be described within the magnetohydrodynamics approximation (cf. Plechaty, Presura & Esaulov 2013; Priest 2014; Moritaka *et al.* 2016; Srivastava *et al.* 2019; Patel *et al.* 2021). In the laser and cosmic plasmas with weak, rare collisions of particles, the leading mechanism of the formation of relatively small-scale current structures is the Weibel instability (Weibel 1959; Davidson 1989; Kocharovsky *et al.* 2016; Borodachev *et al.* 2017). It is caused by the anisotropy of the charged particle velocity distribution and can initiate or change various transient processes involving the generation of strong small-scale magnetic fields.

In this work we continue our recent studies (Nechaev *et al.* 2020*a*,*b*) of the Weibel instability during the decay of a strong discontinuity in the density and temperature of a non-relativistic plasma with hot electrons by means of numerical simulations using the code EPOCH (Arber *et al.* 2015). Investigating the plasma expansion into vacuum (in this case the electrostatic shock wave does not form), we focus mainly on the role of a uniform external magnetic field that is parallel to the plane boundary of the plasma and oriented either along or across the inhomogeneously heated region elongated along this boundary. To the best of our knowledge, the decay of a magnetized plasma–vacuum discontinuity in this geometry has not been studied in detail (cf. Thaury *et al.* 2010; Dieckmann *et al.* 2018; Fox *et al.* 2018; Schoeffler & Silva 2018; Moreno *et al.* 2020), although under other conditions the Weibel-type instabilities and, in particular, the filamentation instability have been frequently investigated numerically, e.g. for colliding plasma flows, including magnetized ones (see Silva 2006; Chang, Spitkovsky & Arons 2008; Spitkovsky 2008; Bret 2009; Dieckmann 2009; Sironi & Spitkovsky 2009; Sironi, Spitkovsky & Arons 2013; Ruyer, Gremillet & Bonnaud 2015).

The strongly non-equilibrium expansion of a magnetized plasma from an initially heated region is possible only if the energy density of an external magnetic field $B_0$ is less than or of the order of the kinetic energy density of the hot electrons. Let $n_0$ and $T$ denote the initial number density and isotropic temperature (in energy units) of the hot electrons, respectively. In the limit $B_0^2/8\pi \ll n_0 T$, the field weakly affects the profile of the expanding plasma density, but can significantly influence the arising anisotropy of the electron velocity distribution and the accompanying Weibel-type instability. In the considered geometry, the latter can develop even in the absence of an external field.

The contents of the paper are as follows. Section 2 describes the initial geometry of the plasma–vacuum discontinuity in our PIC simulations of its decay in the presence of an external magnetic field of various orientations. A typical example of the results

https://doi.org/10.1017/S0022377822000423 Published online by Cambridge University Press

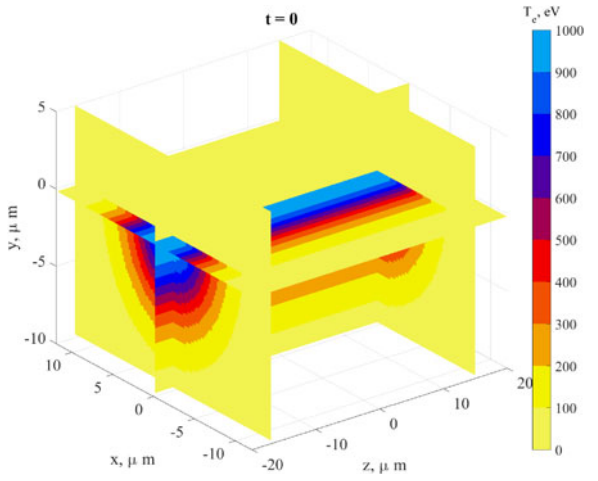


FIGURE 1. Geometry of a semicylindrical cloud (below the target surface $y = 0$) of heated electrons and their initial temperature distribution in the PIC simulations.

of the three dimension-in-space and three dimension-in-velocity (3D3V) simulations of this plasma discontinuity decay is presented in § 3. Section 4 describes the main features of such a decay which are clarified by means of two dimension-in-space and three dimension-in-velocity (2D3V) simulations for a representative set of the external magnetic fields and various plasma densities. In § 5 we discuss the revealed qualitative patterns and some open problems of the phenomenon in question. General conclusions are stated in § 6.

## 2. An initial-value problem of the plasma–vacuum discontinuity decay in the case of a semicylindrical region of heated electrons

Bearing in mind a typical laser-ablation experiment, at the initial moment of time we choose the following density and temperature of ions (with a mass of $M = 100\,m$, where $m$ is the electron mass), placed below the plane $y = 0$ in Cartesian coordinates: $n(y > 0) = 0$, $n(y \le 0) = n_0 = 1.7 \times 10^{22}$, $10^{21}$ or $10^{20}\,\mathrm{cm}^{-3}$ (in different simulations) and $T_i = 10\,\mathrm{eV}$. We take the initial temperature of heated Maxwellian electrons (see figure 1) to be independent of the coordinate $z$ and vary with the radius according to the Gaussian law with the maximum temperature $T = 1\,\mathrm{keV}$ at the point $x = 0$, $y = 0$ and the asymptotic value $T_{e,\infty} = T_i = 10\,\mathrm{eV}$ at a large distance $r = (x^2 + y^2)^{1/2}$ from that point: $T_e = T_{e,\infty} + (T - T_{e,\infty})\exp(-r^2/r_0^2)$. We assume that $r_0 = 25\,\mu\mathrm{m}$ in the simulations with $n_0 = 10^{20}$, $10^{21}\,\mathrm{cm}^{-3}$ and $r_0 = 5\,\mu\mathrm{m}$ in the simulations with $n_0 = 1.7 \times 10^{22}\,\mathrm{cm}^{-3}$. The geometry of this temperature distribution corresponds to a long semicylinder that has the axial section lying on the surface of the plasma, $y = 0$, and the axis directed along the $z$-axis. The external magnetic field $\boldsymbol{B}_0$ is directed along either the $y$- or $z$-axis.

Below we describe the results of typical simulations and the revealed physical phenomena for the initial density of heated electrons $n_0$ (equal to the density of ions) within the $10^{21}$–$1.7 \times 10^{22}\,\mathrm{cm}^{-3}$ range for strong external magnetic fields in the range of 13–2500 T and a lower density, $n_0 = 10^{20}\,\mathrm{cm}^{-3}$, for milder fields in the range of 0.5–13 T. A typical field value of 13 T is chosen based on the parameters of the experiment planned in the Institute of Applied Physics of the Russian Academy of Sciences where an observation of the multiscale magnetic field structures is possible. For the indicated densities, according to estimates (see also § 4), the external fields less than 1 T and 0.1 T,

https://doi.org/10.1017/S0022377822000423 Published online by Cambridge University Press

respectively, have little effect on the energy and structure of the magnetic fields generated in the plasma. The external fields above 2500 T and 200 T, respectively, practically exclude the explosive decay of a hot plasma discontinuity with the parameters mentioned above.

Particle-in-cell simulations using the EPOCH code (Arber *et al.* 2015) are carried out either as completely 3D3V with periodic boundary conditions at $z = \pm L_z/2$ (with $L_z = 40\,\mu\text{m}$) or simplified 2D3V, omitting all dependencies on the coordinate $z$, but still taking into account all three components of all vectors (including the particle velocity vectors). In the latter case, the $z$-axis is directed across the computational plane $xy$ and the development of the Weibel instability or the plasma-boundary currents, as a rule, leads to the formation of filaments or current sheets elongated mainly along this $z$-axis. On the side boundaries of the computational domain ($x = \pm L_x/2$), parallel to the $y$-axis, the periodic boundary conditions for particles and fields are used. The lower boundary ($y = -L_y/4$) reflects particles but allows the fields to escape (be absorbed). The upper boundary ($y = 3L_y/4$) is open for both particles and fields. The dimensions are $L_x \times L_y = 240 \times 240\,\mu\text{m}^2$ for the density $n_0 = 10^{20}$, $10^{21}\,\text{cm}^{-3}$ and $L_x \times L_y = 36 \times 36\,\mu\text{m}^2$ for the density $n_0 = 1.7 \times 10^{22}\,\text{cm}^{-3}$.

The plasma comprises $2.5 \times 10^9$ ($2 \times 10^8$) macroparticles of each fraction, electrons and ions, in 3D3V (2D3V) calculations and the computational domain consists of $400 \times 400 \times 400$ ($1200 \times 1200$) cells. The simulation duration is mainly limited by the moment of time $\tau_\text{R} = 6 \times 10^4 \omega_{pe}^{-1}$ when the transient phenomena have been already fully manifested but the qualitative differences between the 3D3V and simplified 2D3V calculations have not yet usually arisen. Here $\omega_{pe} = (4\pi e^2 n_0/m)^{1/2}$ is the plasma frequency and $e$ is the elementary charge. We have $\tau_R \approx 8$ and 100 ps for $n_0 = 1.7 \times 10^{22}$ and $10^{20}\,\text{cm}^{-3}$, respectively. The skin depths are $c/\omega_{pe} \approx 0.04$ and $0.5\,\mu\text{m}$, respectively, and do not appear in our simulations, so that the observed phenomena are not related to this scale.

For the chosen parameters, particle collisions are weak in the rarefied plasma regions of interest where the expansion into the vacuum (towards $y > 0$) and the formation of currents take place. Indeed, already for the densities of $0.1n_0 = 10^{19}$, $1.7 \times 10^{21}\,\text{cm}^{-3}$ the mean free path of hot electrons, $L_f$, is within the range 5000–50 μm, thus greater than $r_0$, $L_{x,y}$ and a typical size of the region where the small-scale magnetic fields are formed (see, e.g. figures 2–7). Particle collisions are significant in the dense plasma below the target surface where the collisionless PIC simulations may not be valid.

## 3. Three-dimensional simulation for a typical set of plasma parameters with the external magnetic field parallel to the elongated heated region

Due to a lack of room, we illustrate a full 3-D calculation by just one figure, i.e. figure 2. Figure 2(*b*) shows a typical tufted structure of the transverse component of the self-generated magnetic field $B_\perp = (B_x^2 + B_y^2)^{1/2}$ at a high initial density $n_0 = 1.7 \times 10^{22}\,\text{cm}^{-3}$ of hot electrons with an average temperature $T \sim 0.5\,\text{keV}$ and a strong external magnetic field $B_{0z} = 250\,\text{T}$ directed along the axis $z$ of the heated semicylinder. This distribution of the field is created by the electric current filaments, on average parallel to $z$ and shown in figure 2(*a*). At the short time $t = 3.0\,\text{ps}$ after the expansion begins, there is only a small semicylinder with a radius less than 3 μm where the longitudinal self-generated field $B_z - B_{0z}$ is of the order of (and directed opposite to) the external field. At this time and during further expansion at the picosecond time scale, when the plasma pressure dominates over the magnetic one, the displacement of the external field by the large-scale transverse electron currents (as in a solenoid) occurs approximately with an ion-acoustic speed $\propto (T/M)^{1/2} \sim 10^6\,\text{m s}^{-1}$, i.e. the deceleration of the plasma flow in

https://doi.org/10.1017/S0022377822000423 Published online by Cambridge University Press

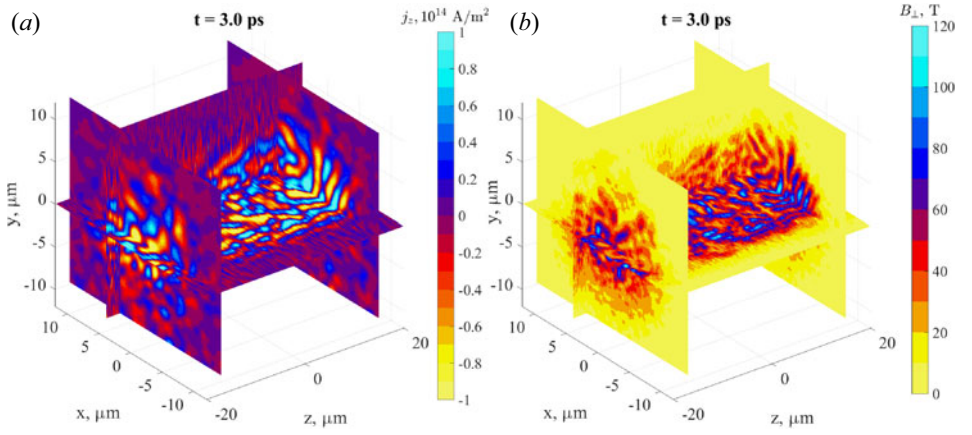


FIGURE 2. (*a*) The current density component $j_z$ representing the self-generated filamentary structure that is mostly aligned with the $z$-axis and (*b*) the magnitude of the transverse magnetic field, $(B_x^2 + B_y^2)^{1/2}$, from the 3-D PIC simulation of the expansion of the plasma cloud with hot electrons into vacuum at the moment of time $t = 3.0\,\mathrm{ps} \approx 3 \times 10^4 \omega_{pe}^{-1}$. The initial plasma density is $n_0 = 1.7 \times 10^{22}\,\mathrm{cm}^{-3}$. The external magnetic field is oriented along the $z$-axis, $\boldsymbol{B}_0 \| Oz$, $B_{0z} = 250\,\mathrm{T}$.

the $xy$-plane only slightly exceeds its deceleration in the absence of the external field. (In actual experiments with heavier ions of $M \sim 50\,000\,\mathrm{m}$ and higher electron temperatures of $T \sim 5\,\mathrm{keV}$, the plasma will expand with a smaller ion-acoustic speed $\sim 10^5\,\mathrm{m\,s}^{-1}$.)

Hereafter, attention should be paid first of all to the rather universal effect of a small-scale structuring, in particular pinching, of electric currents and the magnetic fields generated by them due to the Weibel-type instability, which itself results from the growth of the electron velocity distribution anisotropy in the non-equilibrium plasma expanding into vacuum. Namely, the temperature of electrons along the $z$-axis practically does not change for a long time, while their temperature in the transverse $xy$-plane decreases rather rapidly and significantly (this is a 3-D version of the mechanism originally proposed in Thaury *et al.* (2010) and further studied in Nechaev *et al.* (2020*a*)). The instability has the maximum growth rate for the perturbation wavevectors orthogonal to the direction of the maximum electron temperature (the $z$-axis here), and the growth rate decreases (Vagin & Uryupin 2014) with a decrease of the angle between a wavevector and the $z$-axis. So, at later times when the growth of the $z$-oriented filaments is saturated due to the self-generated magnetic field, the oblique filaments become quite pronounced and the entire current structure becomes more irregular and strongly dependent on the $z$-coordinate. It is already shown in figure 2(*a*) where there are some oblique filaments of finite lengths, especially in the centre region of the expanding plasma.

We justify this conclusion on the Weibel-type mechanism of the growth and saturation of the small-scale current filaments by comparing the gyroradius and gyrofrequency of hot electrons in the self-generated magnetic field with the scale of inhomogeneity and the growth rate of the magnetic field characteristic of the Weibel instability (Vagin & Uryupin 2014; Kocharovsky *et al.* 2016; Nechaev *et al.* 2020*a*). As the simulations show, in the region of interest, $0 < y < 5\,\mu\mathrm{m}$ (see figure 2), the plasma density and the longitudinal electron temperature are $n_e \sim 0.1 n_0 \approx 1.7 \times 10^{21}\,\mathrm{cm}^{-3}$ and $T_z \sim 0.5\,\mathrm{keV}$, respectively. Adopting also the observed values of the self-generated transverse field $\sim$50 T and the

https://doi.org/10.1017/S0022377822000423 Published online by Cambridge University Press

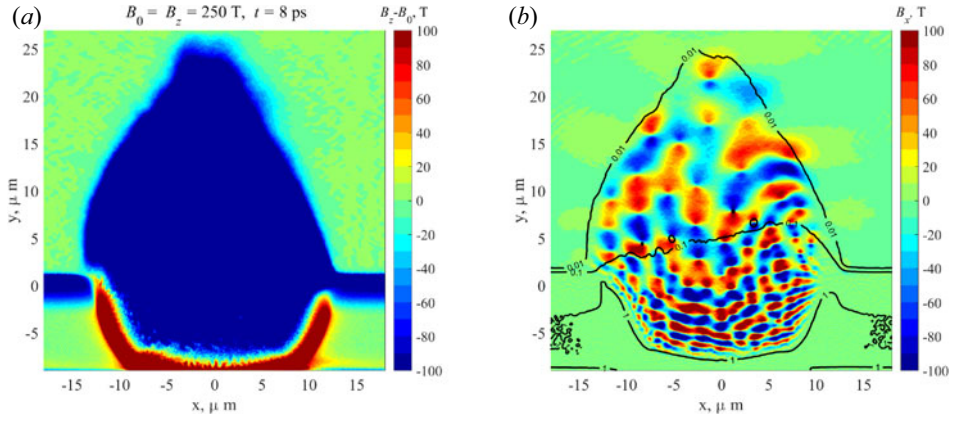


FIGURE 3. Magnetic field structures generated in the 2-D simulation of the expansion of the plasma cloud with hot electrons into vacuum at $t = 8\,\mathrm{ps} \approx 6 \times 10^4 \omega_{pe}^{-1}$ after the beginning of the expansion. The initial plasma density is $n_0 = 1.7 \times 10^{22}\,\mathrm{cm}^{-3}$. The external magnetic field is $B_0 = 250\,\mathrm{T}$ and orthogonal to the simulation plane, $\boldsymbol{B}_0 \| Oz$. (*a*) $B_z$ component of the total magnetic field minus the external magnetic field. (*b*) The $B_x$ component of the magnetic field; black contours show the isolines of the normalized density for $n/n_0 = 0.01, 0.1, 1$.

temperature anisotropy $A = T_z/T_x - 1 \sim 1$, we find that the gyroradius of a hot electron, $r_B = (2T_z/m)^{1/2}\omega_B^{-1} \approx 1.5\,\mu\mathrm{m}$, is approximately equal to the optimal scale of the electron Weibel instability, $\lambda \sim 10c/\omega_{pe}\ (n_0/n_e)^{1/2}A^{-1/2} \sim 1.4\,\mu\mathrm{m}$, and its gyrofrequency $\omega_B \approx 9 \times 10^{12}\,\mathrm{rad\,s}^{-1}$ is close to the maximum Weibel growth rate $\Gamma \sim 3\ (T_x/m)^{1/2}\lambda^{-1}(1 + A^{-1})^{-1} \sim \omega_{pe}/900 \sim 8 \times 10^{12}\,\mathrm{s}^{-1}$. Hence, the magnetic field value satisfies the well known saturation condition for the Weibel instability (see, e.g. Kocharovsky *et al.* 2016). Its characteristic growth time $\tau_B$ in simulations is also consistent with the Weibel mechanism: $\tau_B \sim 10\Gamma^{-1}$. According to the next section, similar qualitative conclusions ($\lambda \sim r_B$ and $\tau_B \sim 10\Gamma^{-1}$) follow from the 2-D simulations (figure 3), which have been compared with the 3-D simulations and shown to be correct with respect to the main features of the small- and large-scale structures of the generated magnetic fields.

Also noticeable is the cumulation (focusing) of the plasma flow, formed collectively by the hot electrons and the cold ions, in the direction of the maximum deformation of the magnetic field lines in the region of the greatest pressure of escaping electrons. The cumulation takes place when this field is oriented along the long heated region on the target surface as is discussed in the next section (see figure 3). Note that in all of these simulations the dynamics of electric currents is quasi-static, since the evolution time of the characteristic structures exceeds the scale of their inhomogeneity divided by the velocity of typical particles, and the role of the induction electric field is inessential.

## 4. Two-dimensional simulations for a wide range of the plasma density and external magnetic field values. A comparative analysis

The established validity of the simplified 2D3V calculations for a qualitative analysis of physical phenomena at a considerably long period of the decay of the plasma discontinuity with an elongated (semicylindrical) region of heated electrons, allows us to describe in more detail a number of features of this process at various plasma densities as well as various values and orientations of an external magnetic field. It is convenient to illustrate these features by comparing figures 3–7.

https://doi.org/10.1017/S0022377822000423 Published online by Cambridge University Press

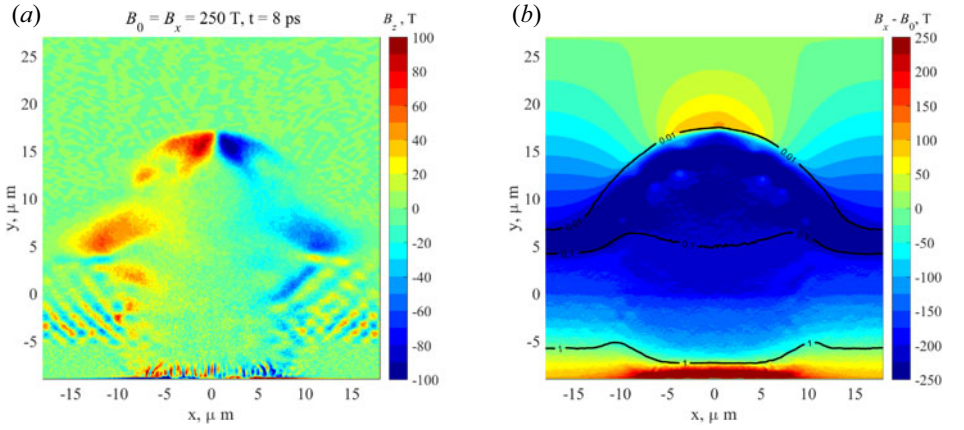


FIGURE 4. Magnetic field structures generated in the 2-D simulation of the expansion of the plasma cloud with hot electrons into vacuum at $t = 8$ ps after the beginning of the expansion. The initial plasma density is $n_0 = 1.7 \times 10^{22}$ cm$^{-3}$. The external magnetic field is $B_0 = 250$ T and lies in the simulation plane, $\boldsymbol{B}_0 \| Ox$. (*a*) $B_z$ component of the magnetic field. (*b*) The $B_x$ component of the total magnetic field minus the external magnetic field; black contours show the isolines of the normalized density for $n/n_0 = 0.01, 0.1, 1$.

First of all, it is clear from figures 2–4 and 7 that, in the region of the expanding collisionless plasma cloud, the magnetic field could substantially weaken or significantly change its direction and even become directed opposite to the external one, keeping almost the same order of magnitude ($\sim B_0/3$). Moreover, under certain conditions, according to the laws of magnetostatics, in the outside boundary region next to the expanding cloud (practically in vacuum) the magnetic field can also change its direction and even increase, differently in different regions and depending on the strength of the local quasi-surface currents and the orientation of the external magnetic field. At the same time, for both orthogonal orientations of the external field ($B_{0z}$ and $B_{0x}$), there is an axial asymmetry, i.e. a difference in directions of the generated magnetic fields, especially near the initial plasma discontinuity to the left and to the right with respect to the centre of the heated section. This asymmetry arises due to the vertical, parallel to the *y*-axis, component of the electric current created by the central 'fountain' of the escaping electrons and the currents flowing in the dense plasma and compensating the charge of these escaped electrons, as can be seen from the magnetic field distributions in figures 3(*b*) and 4(*a*) (on the 'fountain' mechanism in the absence of an external magnetic field, as in figure 6, see, e.g. Kolodner & Yablonovitch (1979), Sakagami *et al.* (1979) and Albertazzi *et al.* (2015)).

According to the simulations, the resulting structure of the electric currents and quasi-magnetostatic fields is practically independent of an external magnetic field only if the latter is very weak ($B_0 < 0.1$ T and $B_0 < 1$ T for the chosen plasma parameters with the initial hot electron density of $n_0 = 10^{20}$ cm$^{-3}$ and $1.7 \times 10^{22}$ cm$^{-3}$, respectively). Such a weak field is easily displaced by the plasma and does not essentially change an electron distribution function. If the external magnetic field is stronger, though still satisfies the inequality $B_0^2/8\pi \ll n_0 T$ and is displaced by the plasma, then the electron distribution function in a considerable volume of a plasma cloud is significantly changed during the plasma expansion. Nevertheless, the Weibel instability will proceed qualitatively similar to that in the absence of the external field, if both the electron gyrofrequency $eB_r/(mc)$ for the remaining in the region (after the displacement) average magnetic field $B_r$ and the

https://doi.org/10.1017/S0022377822000423 Published online by Cambridge University Press

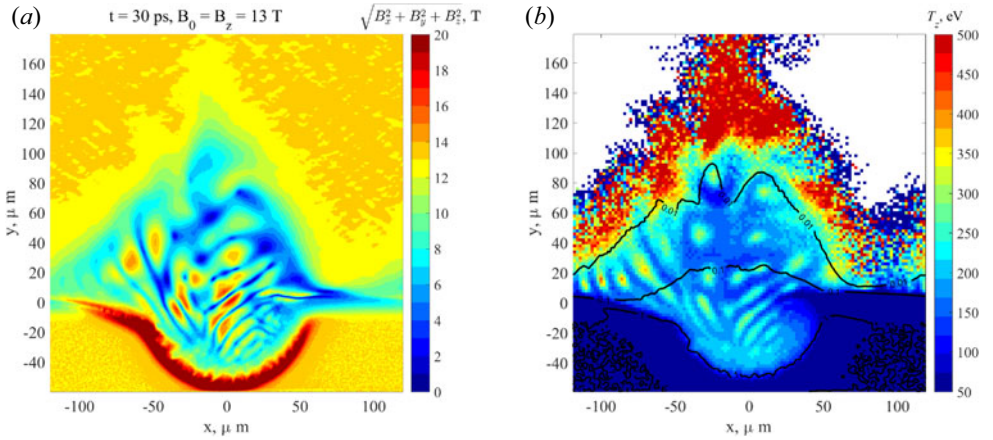


FIGURE 5. The expansion of the plasma cloud with hot electrons (with the initial density of $n_0 = 10^{20}\,\mathrm{cm}^{-3}$) into vacuum with the external magnetic field $B_0 = 13\,\mathrm{T}$, $\boldsymbol{B}_0 \| Oz$, at $t = 30\,\mathrm{ps}$ $\approx 2 \times 10^4 \omega_{pe}^{-1}$ after the beginning of the expansion. (*a*) The magnitude of the total magnetic field. (*b*) The effective temperature $T_z$ along the $z$-axis; black contours show the isolines of the normalized density for $n/n_0 = 0.01, 0.1, 1$.

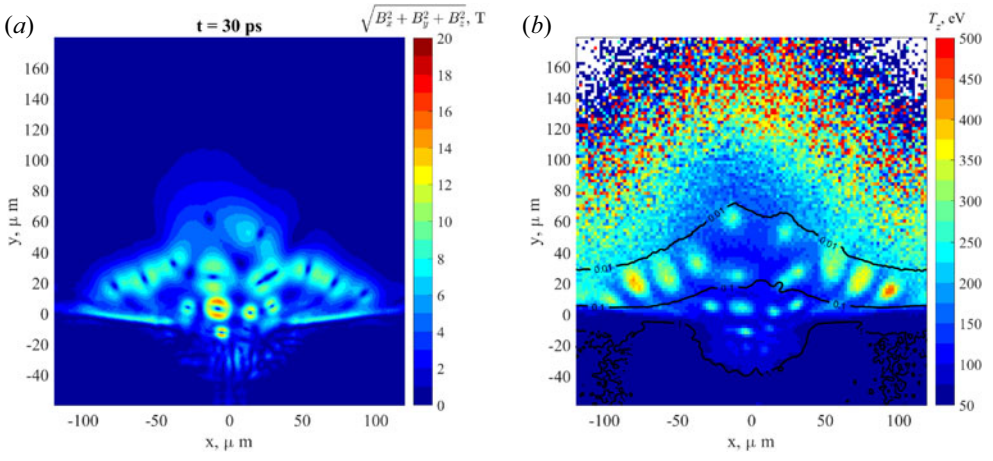


FIGURE 6. The expansion of the plasma cloud with hot electrons (with the initial density of $n_0 = 10^{20}\,\mathrm{cm}^{-3}$) into vacuum without an external magnetic field at $t = 30\,\mathrm{ps}$ after the beginning of the expansion. (*a*) The magnitude of the total magnetic field. (*b*) The effective temperature $T_z$ along the $z$-axis; black contours show the isolines of the normalized density for $n/n_0 = 0.01, 0.1, 1$.

inverse gyroradius of energetic electrons in this field are sufficiently (logarithmically) less than the maximum growth rate and the corresponding wavenumber of the instability in the anisotropic expanding plasma, respectively. Otherwise, the instability is influenced by the remaining large-scale inhomogeneous magnetic field which depends on the orientation of the external field and is comparable to the Weibel saturation field. As a result, the structure of the self-generated magnetic field during the decay of the discontinuity will differ considerably from that in the absence of an external field (figure 6).

The resulting profile of the ejected plasma cloud is almost independent of even stronger external fields for any of their orientations, e.g. for the values $B_{0z}$, $B_{0x}$ under 13 T at the

https://doi.org/10.1017/S0022377822000423 Published online by Cambridge University Press

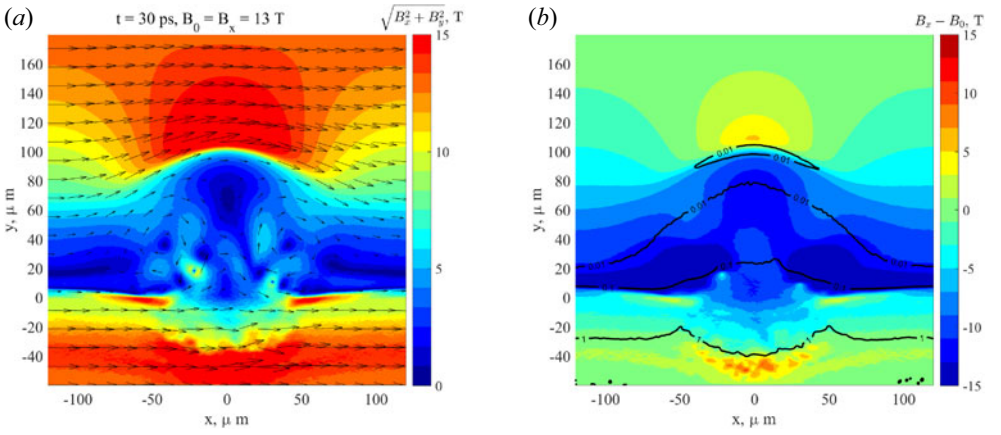


FIGURE 7. The expansion of the plasma cloud with hot electrons (with the initial density of $n_0 = 10^{20}\,\mathrm{cm}^{-3}$) into vacuum with the external magnetic field $B_0 = 13\,\mathrm{T}$, $\boldsymbol{B}_0 \| Ox$, at $t = 30\,\mathrm{ps}$ after the beginning of the expansion. (*a*) The magnitude of the total in-plane magnetic field; arrows show the direction of the in-plane field component. (*b*) The $B_x$ component of the total magnetic field minus the external magnetic field; black contours show the isolines of the normalized density for $n/n_0 = 0.01, 0.1, 1$.

density of $n_0 = 1.7 \times 10^{22}\,\mathrm{cm}^{-3}$. However, upon reaching the indicated (see figures 5 and 7 for $n_0 = 10^{20}\,\mathrm{cm}^{-3}$) and larger values (for example, $B_{0z}$, $B_{0x} = 250\,\mathrm{T}$, as in figures 3 and 4 for $n_0 = 1.7 \times 10^{22}\,\mathrm{cm}^{-3}$), the cases of orientation of the external field along and across the semicylinder of heated electrons begin to differ significantly. In the first case, the aforementioned cumulative effect takes place and, as a result, the rate of the displacement of this field is significantly higher (for example, almost by 1.5 times at $B_{0z} = 250\,\mathrm{T}$) and the plasma cloud is narrower (also almost by 1.5 times at $B_{0z} = 250\,\mathrm{T}$) than in the case of the same-magnitude field $B_{0x}$ orthogonal to the heated semicylinder. In the latter case, the field $B_{0x}$ flattens the plasma cloud via a formation of a completely different system of the large-scale electric currents. In addition, only when the external field is oriented along the $z$-axis is there a noticeable violation of the symmetry of expansion caused by a systematic displacement of a large fraction of electrons to the left under the action of the Lorentz force (directed mainly opposite to the $x$-axis), see figures 3 and 5. At the same time, only when the external field is oriented along the $x$-axis, a formation of the large-scale currents predominantly directed along the $z$-axis takes place at the top of the ejected plume. As a result, they stretch and smoothly bend the magnetic field lines in the $xy$-plane and significantly enhance the external magnetic field in vacuum above the plasma plume, see figures 4(*b*) and 7(*b*).

Our calculations reveal small-scale structures of electron currents flowing mainly parallel to the $z$-axis in the form of Z-pinches with a wide range of transverse scales $\sim$2–50 μm (deformed by the plasma density gradient). They gradually drift along with the plasma in the course of its expansion and give rise to an inhomogeneous set of dipole spots in the structure of the transverse magnetic field components $B_x$, $B_y$ (minus the external field $B_{0x}$, if any; see figures 3*b* and 4*b*). The observed phenomenon is due to the Weibel instability owing to the anisotropically cooling hot electrons, whose effective temperature rapidly decreases along the $x$- and $y$-axes during the discontinuity decay and changes more slowly along the $z$-axis because of an unlimited length of the initially heated plasma semicylinder (cf. Thaury *et al.* 2010). The typical patterns of the electron anisotropy in

https://doi.org/10.1017/S0022377822000423 Published online by Cambridge University Press

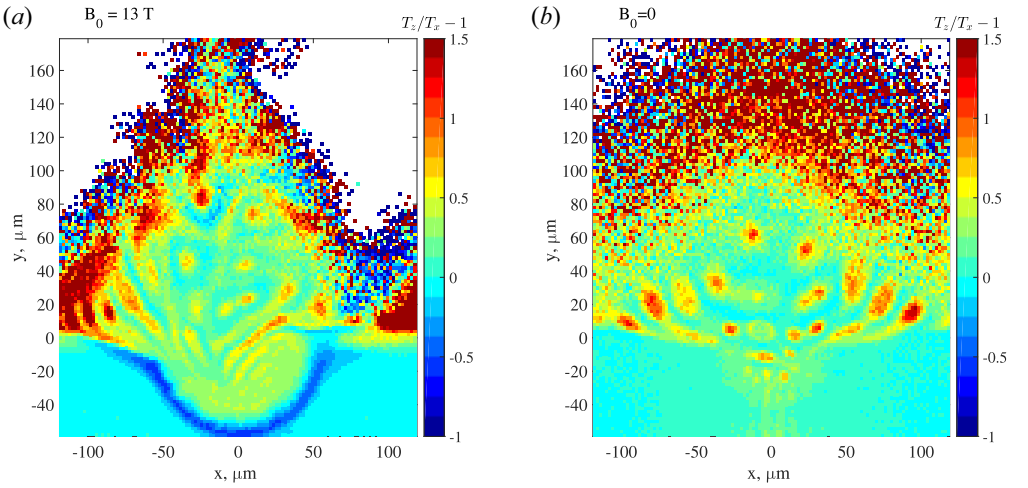


FIGURE 8. The temperature anisotropy degree, $A = T_z/T_x - 1$, induced by the expansion of the plasma cloud with hot electrons (with the initial density of $n_0 = 10^{20}\,\mathrm{cm}^{-3}$) into vacuum (*a*) with the external magnetic field $B_0 = 13\,\mathrm{T}$, $\boldsymbol{B}_0 \| Oz$, (*b*) without an external magnetic field, both at the moment of time $t = 30\,\mathrm{ps} \approx 2 \times 10^4 \omega_{pe}^{-1}$ after the beginning of the expansion.

the cases with and without the external magnetic field $B_{0z}$ are shown in figure 8. The anisotropy degree is quite strong, $A \sim 1$, and the external field $B_{0z} = 13\,\mathrm{T}$ does not inhibit the formation of a set of Z-pinches, though introduces an asymmetry and slows down a bit the plasma expansion. The appearance of the small-scale current filaments, similar to Z-pinches, can be prevented by the strong external field $B_{0x}$ during the displacement of which the large-scale currents along the $z$-axis are generated in the plasma cloud and, as a result, the growth of the temperature anisotropy of the cooling electron distribution is suppressed.

On the contrary, the presence of the external field $B_{0z}$ does not prevent the anisotropic cooling of electrons, so that, from the very beginning of the discontinuity decay, a formation of the multiple-pinch-like current structures occurs (see figure 4*b* for the $x$-component of the quasi-magnetostatic turbulent field created by them as well as figure 5*b* for the effective electron temperature $T_z$ along the $z$-axis associated with such a turbulence). The thickness of these Z-pinches turns out to be of the order of the electron gyroradius, and their transverse magnetic fields can be of the order of or exceed the external field $B_{0z}$. In particular, in the case of figure 5, where $n_0 = 10^{20}\,\mathrm{cm}^{-3}$ and $B_{0z} = 13\,\mathrm{T}$, for a typical filament we observe the magnetic field magnitude ∼5–10 T, radius ∼3–5 μm and total current ∼100 A which are an order of magnitude weaker, by two to three times larger and of the same order of magnitude than, respectively, those in the case of figure 3 (or figure 2), where both $n_0 = 1.7 \times 10^{22}\,\mathrm{cm}^{-3}$ and $B_{0z} = 250\,\mathrm{T}$ are larger. The simulations for the intermediate value of the initial plasma density, $n_0 = 10^{21}\,\mathrm{cm}^{-3}$, show qualitatively the same results.

Additional simulations (not provided in this short article) show that an increase of the ion-to-electron mass ratio decreases the ion-acoustic speed, slows down the process of the plasma expansion and proportionally reduces the scale of the current structures being formed, but does not qualitatively change their small-to-large scale hierarchy and evolution. Also, as expected, an insufficient heating of electrons, i.e. the presence of a significant fraction of cold electrons, notably changes the density profile and geometry

https://doi.org/10.1017/S0022377822000423 Published online by Cambridge University Press

of the plasma ejection, the type of deformation and the rate of the displacement of the external field, the number and spatial distribution of the formed small-scale Z-pinches.

## 5. Main qualitative results and some open physical problems

It is clear from the above that the process of the decay of a plasma–vacuum discontinuity with a semicylindrical region of heated electrons elongated along the plasma surface largely depends on the magnitude and direction of the external magnetic field parallel to the discontinuity surface, even if the pressure of this field is much less than the plasma pressure. The hot electrons make a decisive contribution to the latter and strongly affect the evolution and spatial structure of emerging quasi-magnetostatic perturbations of various scales, especially due to the anisotropic cooling during the expansion.

Along with the obvious influence of the sufficiently strong external magnetic field on the density profile of the expanding plasma cloud, it turns out that even a relatively weak external magnetic field can both suppress and promote, depending on its orientation, the formation of various current filaments, sheets and large-scale structures. The performed simulations and estimates allow us to determine the conditions under which the multiple formation, prolonged existence and significant shift of the localized current filaments (similar to Z-pinches) and more complex current configurations take place in the most part of the region swept from the external magnetic field by the expanding plasma.

The resulting current filaments of the Z-pinch type can have a significantly increased plasma density and create small-scale magnetic fields which turn out to be of the order of or even stronger than the external field and contain approximately several per cent of the initial energy of hot electrons. This occurs in those spatiotemporal regions where the plasma density and the anisotropy of the electron velocity distribution are sufficiently high and promote the development of the Weibel-type instability until its nonlinear saturation, as well as a long-term existence of the entire current structures.

The formation of magnetic fields with a larger scale, of the order of the characteristic transverse size of the elongated heated plasma region, is caused by both the initially strongest ‘fountain’ currents of the fastest escaping electrons as well as by the rapidly generated volumetric or quasi-2-D currents of the hot electrons moving inside the inhomogeneously expanding plasma cloud and along its boundary with the unperturbed external magnetic field. Interacting with this larger-scale current structure, the unidirectional external magnetic field oriented transverse to the main flow of the hot electrons can lead to not just a violation of the symmetry of the expansion, but also to a cumulation of the plasma flow and an inhomogeneous deformation of the emerging multiscale current structures.

We considered just the simplest possible model of the expansion of an inhomogeneously heated magnetized plasma with a uniform density, bearing in mind an ideal cylindrical lens and an ideal target subjected to an ablation by a femtosecond laser beam. Obviously, rather different (not quasi-one-dimensional) distributions of the density and effective temperatures of the rapidly heated electrons are possible if they are exposed to ultrashort laser pulses of various duration, cross-section, polarization and optical frequency. Moreover, the velocity distribution function of electrons could be non-Maxwellian and anisotropic at the very beginning of the expansion. In the actual experiments, a non-planar initial geometry of the interface between a heated plasma and vacuum or a background plasma, particle collisions and an inflow of hot electrons from deeper heated regions of the target – all of which we did not take into account – could also be important. These and other factors related to the planned experiments on the plasma discontinuity decay in an external magnetic field will be addressed elsewhere.

The obtained results can find applications in the topical studies of the astrophysical objects as well as the high-energy density laboratory plasma systems. The described transient phenomena of the self-consistent growth and nonlinear evolution of the small- and large-scale magnetic field structures are particularly relevant to the dynamics of the solar flares, stellar wind formation and non-stationary structure of planetary magnetosheath regions; (see, e.g. Kelley (2009), Dudık *et al.* (2017), Vörös *et al.* (2017), Balogh *et al.* (2018), DeForest *et al.* (2018), Viall & Borovsky (2020) and Lazar *et al.* (2022)). Discussions of the related kinetic phenomena in the physics of cosmic plasma are beyond the scope of the present paper.

## 6. Conclusions

The results presented above show that the character of the expansion of a collisionless electron–ion plasma into vacuum and the currents and magnetic fields of various scales generated in the transition layer depend significantly on the geometry of the region of initially heated electrons and the magnitude and direction of the external magnetic field oriented along the plasma surface. We carried out the detailed numerical (i.e. PIC) analysis for a region with initially isotropically heated electrons in the form of a long semicylinder, the axis of which is located on the plasma surface. This analysis discloses a crucial role of the Weibel-type instabilities that are associated with the emerging anisotropy of the electron velocity distribution and strongly depend on the orientation of the external magnetic field.

We reveal, under certain conditions, a formation and a rapid expansion of highly inhomogeneous electron currents in the form of filaments (similar to Z-pinches) parallel to the external magnetic field as well as a formation and a slow evolution of current sheets oriented at different angles to the boundary between the plasma and the deformed magnetic field. We find that these currents can create fields significantly exceeding in magnitude the external magnetic field and indicate qualitatively the conditions on the magnitude and orientation of the latter as well as on the plasma parameters and electron heating required for this to occur. The predicted phenomena of the decay of the plasma discontinuity are feasible not only in the laser plasma but also in the coronal arches, stellar wind and explosive processes in the planetary magnetospheres.

## Acknowledgements

*Editor V. Malka thanks the referees for their advice in evaluating this article.*

## Funding

The laboratory astrophysics part of the work was supported by the Russian Science Foundation, project no. 21-12-00416. The computations were enabled by resources provided by the Joint Supercomputer Center of the Russian Academy of Sciences.

## Declaration of interests

The authors report no conflict of interest.

## REFERENCES

Albertazzi, B., Chen, S.N., Antici, P., Böker, J., Borghesi, M., Breil, J., Dervieux, V., Feugeas, J.L., Lancia, L., Nakatsutsumi, M., *et al.* 2015 Dynamics and structure of self-generated magnetics fields on solids following high contrast, high intensity laser irradiation. *Phys. Plasmas* **22** (12), 123108.

https://doi.org/10.1017/S0022377822000423 Published online by Cambridge University Press

ARBER, T.D., BENNETT, K., BRADY, C.S., LAWRENCE-DOUGLAS, A., RAMSAY, M.G., SIRCOMBE, N.J., GILLIES, P., EVANS, R.G., SCHMITZ, H., BELL, A.R., *et al.* 2015 Contemporary particle-in-cell approach to laser-plasma modelling. *Plasma Phys. Control. Fusion* **57** (11), 113001.

BALOGH, A., BYKOV, A., EASTWOOD, J. & KAASTRA, J. 2018 *Multi-scale Structure Formation and Dynamics in Cosmic Plasmas*. Springer.

BORODACHEV, L.V., GARASEV, M.A., KOLOMIETS, D.O., KOCHAROVSKY, V.V., MARTYANOV, V.Y. & NECHAEV, A.A. 2017 Dynamics of a self-consistent magnetic field and diffusive scattering of ions in a plasma with strong thermal anisotropy. *Radiophys. Quant. El.* **59** (12), 991–999.

BRET, A. 2009 Weibel, two-stream, filamentation, oblique, bell, Buneman…which one grows faster? *Astrophys. J.* **699** (2), 990–1003.

CHANG, P., SPITKOVSKY, A. & ARONS, J. 2008 Long-term evolution of magnetic turbulence in relativistic collisionless shocks: electron-positron plasmas. *Astrophys. J.* **674** (1), 378–387.

DAVIDSON, R.C. 1989Kinetic waves and instabilities in a uniform plasma. In *Basic Plasma Physics: Selected Chapters from the Handbook of Plasma Physics, vol. 1 and 2* (ed. A.A. Galeev & R.N. Sudan), p. 229. North-Holland.

DEFOREST, C.E., HOWARD, R.A., VELLI, M., VIALL, N. & VOURLIDAS, A. 2018 The highly structured outer solar corona. *Astrophys. J.* **862** (1), 18.

DIECKMANN, M.E. 2009 The filamentation instability driven by warm electron beams: statistics and electric field generation. *Plasma Phys. Control. Fusion* **51** (12), 124042.

DIECKMANN, M.E., MORENO, Q., DORIA, D., ROMAGNANI, L., SARRI, G., FOLINI, D., WALDER, R., BRET, A., D'HUMIÈRES, E. & BORGHESI, M. 2018 Expansion of a radially symmetric blast shell into a uniformly magnetized plasma. *Phys. Plasmas* **25** (5), 052108.

DUDIK, J., DZIFČÁKOVÁ, E., MEYER-VERNET, N., ZANNA, G.D., YOUNG, P.R., GIUNTA, A., SYLWESTER, B., SYLWESTER, J., OKA, M., MASON, H.E., *et al.* 2017 Nonequilibrium processes in the solar corona, transition region, flares, and solar wind (invited review). *Solar Phys.* **292** (8).

FOX, W., MATTEUCCI, J., MOISSARD, C., SCHAEFFER, D.B., BHATTACHARJEE, A., GERMASCHEWSKI, K. & HU, S.X. 2018 Kinetic simulation of magnetic field generation and collisionless shock formation in expanding laboratory plasmas. *Phys. Plasmas* **25** (10), 102106.

GARASEV, M. & DERISHEV, E. 2016 Impact of continuous particle injection on generation and decay of the magnetic field in collisionless shocks. *Mon. Not. R. Astron. Soc.* **461** (1), 641–646.

GÖDE, S., RÖDEL, C., ZEIL, K., MISHRA, R., GAUTHIER, M., BRACK, F.-E., KLUGE, T., MACDONALD, M., METZKES, J., OBST, L., *et al.* 2017 Relativistic electron streaming instabilities modulate proton beams accelerated in laser-plasma interactions. *Phys. Rev. Lett.* **118** (19), 194801.

GRUZINOV, A. 2001 Gamma-ray burst phenomenology, shock dynamo, and the first magnetic fields. *Astrophys. J.* **563** (1), L15–L18.

HUANG, L.G., TAKABE, H. & COWAN, T.E. 2019 Maximizing magnetic field generation in high power laser–solid interactions. *High Power Laser Sci. Engng* **7**, E22.

HUNTINGTON, C.M., FIUZA, F., ROSS, J.S., ZYLSTRA, A.B., DRAKE, R.P., FROULA, D.H., GREGORI, G., KUGLAND, N.L., KURANZ, C.C., LEVY, M.C., *et al.* 2015 Observation of magnetic field generation via the Weibel instability in interpenetrating plasma flows. *Nat. Phys.* **11** (2), 173–176.

KELLEY, M.C. 2009 *The Earth's Ionosphere: Plasma Physics and Electrodynamics*. Academic Press.

KOCHAROVSKY, V.V., KOCHAROVSKY, V.V., MARTYANOV, V.Y. & TARASOV, S.V. 2016 Analytical theory of self-consistent current structures in a collisionless plasma. *Phys.-Usp.* **59** (12), 1165–1210.

KOLODNER, P. & YABLONOVITCH, E. 1979 Two-dimensional distribution of self-generated magnetic fields near the laser-plasma resonant-interaction region. *Phys. Rev. Lett.* **43** (19), 1402–1403.

LAZAR, M., LÓPEZ, R., SHAABAN, S.M., POEDTS, S., YOON, P.H. & FICHTNER, H. 2022 Temperature anisotropy instabilities stimulated by the solar wind suprathermal populations. *Front. Astron. Space Sci.* **8**.

LYUBARSKY, Y. & EICHLER, D. 2006 Are gamma-ray burst shocks mediated by the Weibel instability? *Astrophys. J.* **647** (2), 1250–1254.

MEDVEDEV, M.V. & LOEB, A. 1999 Generation of magnetic fields in the relativistic shock of gamma-ray burst sources. *Astrophys. J.* **526** (2), 697–706.

Moreno, Q., Dieckmann, M.E., Folini, D., Walder, R., Ribeyre, X., Tikhonchuk, V.T. & d'Humières, E. 2020 Shocks and phase space vortices driven by a density jump between two clouds of electrons and protons. *Plasma Phys. Control. Fusion* **62** (2), 025022.

Moritaka, T., Kuramitsu, Y., Liu, Y.-L. & Chen, S.-H. 2016 Spontaneous focusing of plasma flow in a weak perpendicular magnetic field. *Phys. Plasmas* **23** (3), 032110.

Nechaev, A.A., Garasev, M.A., Kocharovsky, V.V. & Kocharovsky, V.V. 2020*a* Weibel mechanism of magnetic-field generation in the process of expansion of a collisionless-plasma bunch with hot electrons. *Radiophys. Quant. El*. **62** (12), 830–848.

Nechaev, A.A., Garasev, M.A., Stepanov, A.N. & Kocharovsky, V.V. 2020*b* Formation of a density bump in a collisionless electrostatic shock wave during expansion of a hot dense plasma into a cold rarefied one. *Plasma Phys. Rep*. **46** (8), 765–783.

Patel, B.G., Behera, N., Singh, R.K., Kumar, A. & Das, A. 2021 A 3D magnetohydrodynamic simulation of the propagation of a plasma plume transverse to applied magnetic field. *Plasma Phys. Control. Fusion* **63** (11), 115020.

Plechaty, C., Presura, R. & Esaulov, A.A. 2013 Focusing of an explosive plasma expansion in a transverse magnetic field. *Phys. Rev. Lett*. **111** (18), 185002.

Priest, E. 2014 *Magnetohydrodynamics of the Sun*. Cambridge University Press.

Quinn, K., Romagnani, L., Ramakrishna, B., Sarri, G., Dieckmann, M.E., Wilson, P.A., Fuchs, J., Lancia, L., Pipahl, A., Toncian, T., *et al.* 2012 Weibel-induced filamentation during an ultrafast laser-driven plasma expansion. *Phys. Rev. Lett*. **108**, 135001.

Romagnani, L., Bulanov, S.V., Borghesi, M., Audebert, P., Gauthier, J.C., Löwenbrück, K., Mackinnon, A.J., Patel, P., Pretzler, G., Toncian, T., *et al.* 2008 Observation of collisionless shocks in laser-plasma experiments. *Phys. Rev. Lett*. **101**, 025004.

Ruyer, C., Bolaños, S., Albertazzi, B., Chen, S.N., Antici, P., Böker, J., Dervieux, V., Lancia, L., Nakatsutsumi, M., Romagnani, L., *et al.* 2020 Growth of concomitant laser-driven collisionless and resistive electron filamentation instabilities over large spatiotemporal scales. *Nat. Phys*. **16** (9), 983–988.

Ruyer, C., Gremillet, L. & Bonnaud, G. 2015 Weibel-mediated collisionless shocks in laser-irradiated dense plasmas: prevailing role of the electrons in generating the field fluctuations. *Phys. Plasmas* **22** (8), 082107.

Sakagami, Y., Kawakami, H., Nagao, S. & Yamanaka, C. 1979 Two-dimensional distribution of self-generated magnetic fields near the laser-plasma resonant-interaction region. *Phys. Rev. Lett*. **42** (13), 839–842.

Sakawa, Y., Morita, T., Kuramitsu, Y. & Takabe, H. 2016 Collisionless electrostatic shock generation using high-energy laser systems. *Adv. Phys.* X **1** (3), 425–443.

Schoeffler, K.M. & Silva, L.O. 2018 General kinetic solution for the Biermann battery with an associated pressure anisotropy generation. *Plasma Phys. Control. Fusion* **60** (1), 014048.

Silva, L.O. 2006 Physical problems (microphysics) in relativistic plasma flows. *AIP Conf. Proc*. **856**, 109–128.

Sironi, L. & Spitkovsky, A. 2009 Particle acceleration in relativistic magnetized collisionless pair shocks: dependence of shock acceleration on magnetic obliquity. *Astrophys. J*. **698** (2), 1523–1549.

Sironi, L., Spitkovsky, A. & Arons, J. 2013 The maximum energy of accelerated particles in relativistic collisionless shocks. *Astrophys. J*. **771** (1), 54.

Spitkovsky, A. 2008 Particle acceleration in relativistic collisionless shocks: Fermi process at last? *Astrophys. J*. **682** (1), L5–L8.

Srivastava, A.K., Mishra, S.K., Jelinek, P., Samanta, T., Tian, H., Pant, V., Kayshap, P., Banerjee, D., Doyle, J.G. & Dwivedi, B.N. 2019 On the observations of rapid forced reconnection in the solar corona. *Astrophys. J*. **887** (2), 137.

Thaury, C., Mora, P., Héron, A. & Adam, J.C. 2010 Self-generation of megagauss magnetic fields during the expansion of a plasma. *Phys. Rev.* E **82** (1), 016408.

Vagin, K.Y. & Uryupin, S.A. 2014 On the growth rate of aperiodic instability in plasma with an anisotropic bi-Maxwellian electron velocity distribution. *Plasma Phys. Rep*. **40** (5), 393–403.

Viall, N.M. & Borovsky, J.E. 2020 Nine outstanding questions of solar wind physics. *J. Geophys. Res*. **125** (7).

VÖRÖS, Z., YORDANOVA, E., VARSANI, A., GENESTRETI, K.J., KHOTYAINTSEV, Y.V., LI, W., GRAHAM, D.B., NORGREN, C., NAKAMURA, R., NARITA, Y., *et al.* 2017 MMS observation of magnetic reconnection in the turbulent magnetosheath. *J. Geophys. Res*. **122** (11), 11442–11467.

WEIBEL, E.S. 1959 Spontaneously growing transverse waves in a plasma due to an anisotropic velocity distribution. *Phys. Rev. Lett*. **2** (3), 83–84.

https://doi.org/10.1017/S0022377822000423 Published online by Cambridge University Press